Table of Contents

List of Abbreviations

Geometric parameters

ϕ	Stagger angle	°
A	Annulus area	m^2
c	Chord (distance between leading edge and trailing edge)	m
c_x	Axial chord, as c projected onto shaft axis	m
D_m	Mean diameter of blade	m
h	Height (blade height between hub and tip)	m
h/c	Blade aspect ratio	-
h/c_x	Axial blade aspect ratio	-
o_t	Throat opening	m
R	Total radius of rotor (axis to tip)	m
R_h	Radius of hub	m
R_m	Mean radius of blade	m
R_t	Radius of tip	m
R_{ht}	Hub-to-tip radius ratio	-
s	Pitch or spacing (distance between two adjacent blades)	m
t	Blade thickness	m
t_{et}	Trailing edge thickness	m
t_{max}	Maximum blade thickness	m

Loss model variabes

$\Delta\phi^2$	Energy loss coefficient for trailing edge losses	-
f_{Re}	Reynolds number correction for profile loss	-

f_{AR}	Aspect ratio correction for secondary loss	-
K_1	Correction term for exit Mach number	-
K_2	Correction term for channel acceleration	-
K_S, K_3	Corrections for subsonic Mach number in secondary losses	-
K_P	Correction term for high Mach numbers	-
K_P, K_1, K_2	Correction terms for loss models	-
Y	Pressure loss coefficient referred to dynamic exit pressure	-
Y_P	Profile loss coefficient	-
Y_S	Secondary loss coefficient	-
Y_{shock}	Profile shock loss coefficient	-
Y_{TC}	Tip clearance loss coefficient	-
Y_{TET}	Trailing edge loss coefficient	-

Subindices and stages

0	Total variable (static + dynamic)
1	Start of turbine stage, entry to vane/stator
2	Stator exit, entry to rotor
3	Rotor exit, end of turbine stage
s	Isentropic value

Thermodynamic variables

ΔH	Enthalpy change	$\mathrm{J\,kg^{-1}}$
η	Isentropic efficiency	-
γ	Heat capacity ratio	
ψ	Stage loading	-
ρ	Static density	$\mathrm{kg\,m^{-3}}$
ρ_0	Total density	$\mathrm{kg\,m^{-3}}$
φ	Flow coefficient or flow function	-
C_p	Heat capacity	

GR	Degree of reaction	-
P	Static pressure	Pa
P_0	Total pressure	Pa
q	Dynamic pressure	Pa
R	Specific gas constant	$\mathrm{J\,kg^{-1}\,K^{-1}}$
T	Static temperature	K
T_0	Total temperature	K
T_s	Ideal static temperature	K

Flow velocities and angles

α_1	Entry angle in vane (between v_1 and shaft axis)	rad
α_2	Exit angle in vane (between v_2 and shaft axis)	rad
α_m	Mean gas angle	rad
β_2	Entry angle in rotor (between w_2 and shaft axis)	rad
β_3	Exit angle in rotor (between w_3 and shaft axis)	rad
Ω	Angular velocity	$\mathrm{rad\,s^{-1}}$
a	Speed of sound	$\mathrm{m\,s^{-1}}$
M	Mach number	
RPM	Revolutions per minute	$\mathrm{rev\,min^{-1}}$
u	Peripheral velocity	$\mathrm{m\,s^{-1}}$
v_u	Tangential component of velocity in fixed axes	$\mathrm{m\,s^{-1}}$
v_x	Axial component of velocity in fixed axes	$\mathrm{m\,s^{-1}}$
w_u	Tangential component of velocity in fixed axes	$\mathrm{m\,s^{-1}}$
w_x	Axial component of velocity in rotating axes	$\mathrm{m\,s^{-1}}$

Chapter 1

Results, test cases, and validation

Once the preliminary research (**??**) and the implementation (chapters **??** and **??**), the resulting design tool must be tested and validated to confirm that it functions correctly in the desired range of applications.

This has been done through two methods. First (section 1.1), several sample design cases have been selected from among existing turbines, as studied in previous research papers. This ensures that all the necessary input data is available, and that the results can be compared and validated.

The second portion of this chapter (section 1.2) contains a series of parametric analysis which were made using the design tool. By establishing a reference case and varying one parameter at a time, the effect of each variable upon the final results is analysed and compared to expected behavior.

The sample cases presented in this chapter, and calculated with the design tool, were performed using the second version of the design tool: that which includes the final convergence loop, but does not place constraints upon the velocities. This was selected because the additional constraints were not needed to find a viable solution in these cases, and the calculation time is significantly higher when the non-linear constraints are enforced. What is more, these values can sometimes impose artificial limits on values which need not be so strictly limited, and have therefore been monitored by the author for these cases.

The sample cases have been selected from various references, so as to compare the generated results to different design methods. Additionally, they have been selected in a range of turbine sizes, confirming the usability of the design tool for a range of turbine applications.

1.1 Sample design problems

1.1.1 Test case 1: Lyulka AL-21 High pressure turbine

The first test case implemented is that of the high-pressure turbine of the **LYULKA AL-21F3** axial flow turbojet engine. This is one of the engines used in the turbine design study completed by Ajoko [1], from which the necessary data has been extracted. All the necessary input parameters are described in that report, and displayed in table 1.1. Although some differences exit between the geometry adopted in this design tool and the reference case (for example, the diverging shape of the rotor), the results will be compared and discussed.

Table 1.1: Inputs for test case 1

Parameter	**Value**	Unit
T_{01}	562.00	K
T_{03}	560.26	K
P_{01}	346.32	kPa
P_{03}	341.57	kPa
$deltaH$	0.18	MJ/kg
$mdot$	25.50	kg/s
GR	0.40	-
psi	2.06	-
R_{ht}	0.98	-

Using the input parameters, the design tool is run for this design case using the generic parameters as discussed in chapters **??** and **??**. Once the calculations are complete, a summary of the results are displayed in a table as is done in [2] (table 1.2), and the resulting velocity triangle shown in figure 1.1.

This turbine is relatively small–the total thrust generated by the jet engine is 110 316 N [3]. Therefore the massflow through the engine is not extremely high, nor are the velocities reached (see figure 1.1) extremely elevated. Notably, the total temperature at the turbine inlet T_{01} is significantly lower than in the next two test cases.

Table 1.2: Results for test case 1

Variable	**Station**					Unit
	1	**2**	**2r**	**3r**	**3**	
\$T_0\$	562	562	493.88	493.88	437.07	K
\$T\$	560.26	479.84	479.84	425.27	425.27	K
\$P_0\$	346.32	332.48	187.13	180.08	104.57	Pa
\$P\$	341.57	164.61	164.61	92.59	92.59	Pa
\$M\$	0.15	1.09	0.45	1.06	0.44	-
\$v\$	66.71	458.08	-	-	173.55	\$m/s\$
\$w\$	-	-	189.03	418.58	-	\$m/s\$
\$alpha\$	0.0	75.0	-	-	-0.6	deg
\$beta\$	-	-	51.16	-70.0	-	deg

The results in the turbine are as expected, with an expansion through both the stator

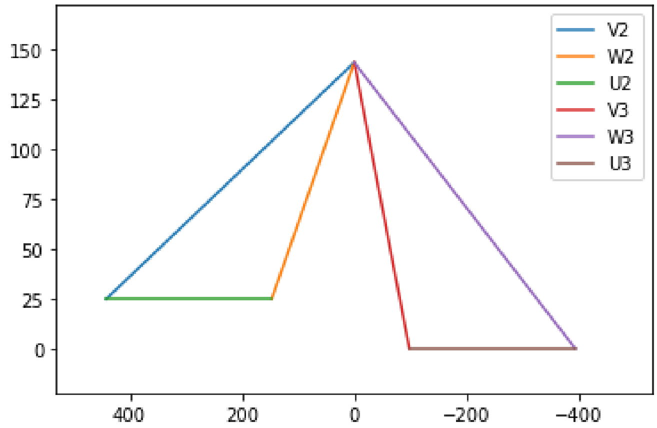

Figure 1.1: FIX AXES LABLES Velocity triangle for the turbine in test case 1

and rotor. Some significant variables can be compared to the results of the reference study, displayed here in table 1.3. As can be seen, the results are extremely similar to those of reference study, varying an average of 7.76% for the variables studied.

Table 1.3: Comparison of results for test case 1 to reference [1]

	eta_{tot}	phi	$DeltaT_0$	A_3	u_m
Design tool	0.9	0.48	124.93	0.23	295.24
Reference	0.9	0.50	118.00	0.25	270.00
Unit	-	-	K	m^2	$m\,s^{-1}$

1.1.2 Initial stage of three-stage high-pressure turbine

1.1.3 Gas generator for automobile

The final case study implemented is for a different kind of turbine: for a gas generator for an automobile, as detailed in a design exercise [4]. At a much smaller scale, the massflow and annulus area is reduced, but the thermodynamic variables such as pressure and temperature are at similar magnitudes to other, larger turbines.

The design exercise referenced provides all the necessary inputs, as seen in table 1.4. The same geometrical assumptions are made in the reference study, and the same processes made in calculation. The differences appear, however, in the calculation of the blade geometry, where the Soderberg correlation is used as an initial estimate of pressure losses.

An additional constraint is added to this case. Since the turbine under design is a single-stage turbine, the exit flow should be as axial as possible, which implies the minimization of the exit swirl angle α_3 (as discussed in **??**). This constraint was added to the angle minimization loop, seen in **??**, along with the total enthalpy constraint. Thus, for this problem in particular, the following constraint is substituted for the general rotor angle

Table 1.4: Inputs for test case 3

Parameter	**Value**	Unit
T_{01}	1400.00	K
T_{03}	1393.53	K
P_{01}	397.19	kPa
P_{03}	389.29	kPa
$deltaH$	0.39	MJ/kg
$mdot$	0.78	kg/s
GR	0.32	-
psi	1.75	-
R_{ht}	0.90	-

constraint:

Rotor angle convergence: find α_2 and β_3 such that both $(\Delta H_{prod} - \Delta H_{calc})$ and $\alpha_3 \rightarrow 0$

Completing the run, the results can be seen in table 1.5 and figure 1.2. As with the other cases, the general behavior is consistent with turbine expansion. Additionally, the exit swirl angle α_3 has been minimized to $-0.38°$, maintaining a nearly complete axial flow at the turbine exit for entry to the nozzle.

Table 1.5: Results for test case 2

Variable	**Station**					Unit
	1	**2**	**2r**	**3r**	**3**	
T_0	1400	1400	1208.3	1208.3	1076.76	K
T	1393.53	1150.23	1150.23	1042.27	1042.27	K
P_0	397.19	354.45	187.25	167.05	101.37	Pa
P	389.29	151.27	151.27	88.03	88.03	Pa
M	0.18	1.2	0.58	1.03	0.47	-
v	126.72	787.03	-	-	292.46	m/s
w	-	-	379.49	641.69	-	m/s
$alpha$	0.0	70.0	-	-	-0.38	deg
$beta$	-	-	44.82	-65.0	-	deg

The results obtained for the turbine in the design tool and the reference study are compared in table 1.6. The results are nearly identical, with an average variation of 1.03%. This is most probably due to the wealth of information available in the sample case. This lowers

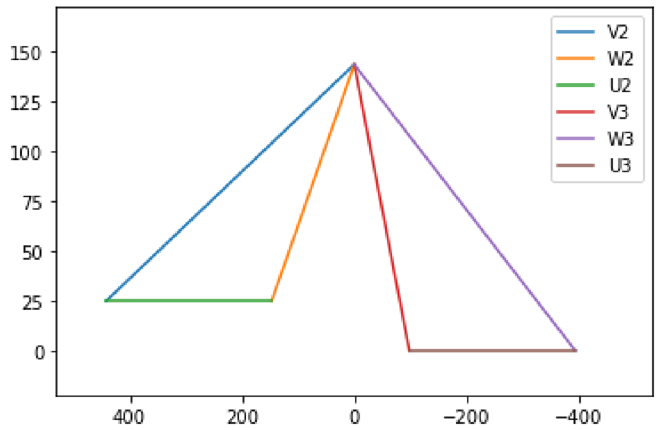

Figure 1.2: REPLACE IMAGE Velocity triangle for the turbine in test case 2

the uncertainty when defining the constraints and initial guesses.

Table 1.6: Comparison of results for test case 2 to reference [4]

	eta_{tot}	phi	A_3	V_3	Y_{stator}	Y_{rotor}
Design tool	0.72	0.52	0.01	254.86	0.22	0.36
Reference	0.72	0.54	0.01	263.92	0.22	0.36
Unit	-	-	m^2	$\mathrm{m\,s^{-1}}$	-	-

1.2 Parametric analyses

1.2.1 Degree of reaction

1.2.2

1.3 Discussion

Chapter 2

Conclusion

(incluyendo, en su caso, líneas de trabajos futuros, y mencionando obligatoriamente las competencias –conocimientos y/o capacidades– del grado que el alumno ha aplicado al TFG y las nuevas competencias –conocimientos y/o capacidades– que el alumno ha adquirido con la realización del TFG)

2.1 Discussion of design tool creation and results

2.2 Personal growth

2.3 Future work

Bibliography

[1] Tolumoye John Ajoko. Design study for single stage high pressure turbine of gas turbine engines. *American Journal of Engineering Research (AJER)*, 03:296–305, 2014.

[2] Jack D. Mattingly. *Elements of propulsion : gas turbines and rockets*. American Institute of Aeronautics and Astronautics, Inc., 2006.

[3] Jet Engine Specification Database. Lyulka al-21f-3, military turbojet/turbofan specification. http://www.jetengine.net/miltfspec.html, 2005.

[4] Jorge Saavedra García. Gas generator for an automobile. Design Exercise, 2013-2014.

[5] Charles R. Harris, K. Jarrod Millman, Stéfan J. van der Walt, Ralf Gommers, Pauli Virtanen, David Cournapeau, Eric Wieser, Julian Taylor, Sebastian Berg, Nathaniel J. Smith, Robert Kern, Matti Picus, Stephan Hoyer, Marten H. van Kerkwijk, Matthew Brett, Allan Haldane, Jaime Fernández del Río, Mark Wiebe, Pearu Peterson, Pierre Gérard-Marchant, Kevin Sheppard, Tyler Reddy, Warren Weckesser, Hameer Abbasi, Christoph Gohlke, and Travis E. Oliphant. Array programming with NumPy. *Nature*, 585(7825):357–362, September 2020.

[6] Pauli Virtanen, Ralf Gommers, Travis E. Oliphant, Matt Haberland, Tyler Reddy, David Cournapeau, Evgeni Burovski, Pearu Peterson, Warren Weckesser, Jonathan Bright, Stéfan J. van der Walt, Matthew Brett, Joshua Wilson, K. Jarrod Millman, Nikolay Mayorov, Andrew R. J. Nelson, Eric Jones, Robert Kern, Eric Larson, C J Carey, İlhan Polat, Yu Feng, Eric W. Moore, Jake VanderPlas, Denis Laxalde, Josef Perktold, Robert Cimrman, Ian Henriksen, E. A. Quintero, Charles R. Harris, Anne M. Archibald, Antônio H. Ribeiro, Fabian Pedregosa, Paul van Mulbregt, and SciPy 1.0 Contributors. SciPy 1.0: Fundamental Algorithms for Scientific Computing in Python. *Nature Methods*, 17:261–272, 2020.

[7] J. D. Hunter. Matplotlib: A 2d graphics environment. *Computing in Science & Engineering*, 9(3):90–95, 2007.

[8] Jeff Reback; jbrockmendel; Wes McKinney; Joris Van den Bossche; Tom Augspurger; Phillip Cloud; Simon Hawkins; gfyoung; Sinhrks; Matthew Roeschke; Adam Klein; Terji Petersen; Jeff Tratner; Chang She; William Ayd; Patrick Hoefler; Shahar Naveh; Marc Garcia; Jeremy Schendel; Andy Hayden; Daniel Saxton; Marco Edward Gorelli; Richard Shadrach; Vytautas Jancauskas; Ali McMaster; Fangchen Li; Pietro Battiston; Skipper Seabold; attack68; Kaiqi Dong. *pandas-dev/pandas: Pandas*. Zenodo, July 2021.

[9] Jorge J. More Burton S. Garbow, Kenneth E. Hillstrom. Documentation for minpack subroutine hybrd. Technical report, Argonne National Laboratory, 1980.

[10] Richard H. Byrd, Mary E. Hribar, and Jorge Nocedal. An interior point algorithm for large-scale nonlinear programming. *SIAM Journal on Optimization*, 9(4):877–900, 1999.

[11] S. C. Kacker and U. Okapuu. A mean line prediction method for axial flow turbine efficiency. *Journal of Engineering for Power*, 104:111–119, 1982.

[12] H. R. M. Craig and H. J. A. Cox. Performance estimation of axial flow turbines. *Proceedings of the Institution of Mechanical Engineers*, 185(1):407–424, 1970.

[13] D.G. Ainley, G.C.R. Mathieson, Aeronautical Research Council London (Great Britain), and Aeronautical Research Council (Great Britain). *A Method of Performance Estimation for Axial-flow Turbines*. Aeronautical Research Council. Reports and memoranda. H.M. Stationery Office, 1951.

[14] J. D. Denton. Loss Mechanisms in Turbomachines. *Journal of Turbomachinery*, 115(4):621–656, 10 1993.

[15] O. Sharma and T. Butler. Predictions of endwall losses and secondary flows in axial flow turbine cascades. *Journal of Turbomachinery*, 109(2):229–236, 04 1986.

[16] P.M. Came J. Dunham. Improvements to the Ainley-Mathieson method of turbine performance prediction. *ASME Journal of Engineering for Power*, 92:252–256, 07 1970.

[17] Giovanni Lozza. A comparison between the craig-cox and the kacker-okapuu methods of turbine performance prediction. *Meccanica*, 17:211–221, 1982.

[18] Daniel Back da Trindade, Pamela Bugała, and Domenico Simone. Review of loss models for high pressure turbines. *Journal of KONES Powertrain and Transport*, 25(2):211–221, 2018.

[19] Ning Wei. *Significance of Loss Models in Aerothermodynamic Simulation for Axial Turbines*. PhD thesis, Journal of KONES Powertrain and Transport, 2000.

[20] Adrian Dahlquist. Investigation of losses prediction methods in 1d for axial gas turbines. Master's thesis, Lund University, 01 2008.

[21] M. Hamidur Rahman, Sung In Kim, and Ibrahim Hassan. Tip leakage flow and heat transfer on turbine blade tip and casing, part 1: Effect of tip clearance height and rotation speed. *International Journal for Computational Methods in Engineering Science and Mechanics*, 14(4):290–303, 2013.

[22] F. J. G. Heyes, H. P. Hodson, and G. M. Dailey. The effect of blade tip geometry on the tip leakage flow in axial turbine cascades. *Journal of Turbomachinery*, 114:643–651, 1992.

[23] Z. Saleh, E. J. Avital, and T. Korakianitis. An investigation into turbine blade tip leakage flows at high speeds. *International Journal of Aerospace and Mechanical Engineering*, 7(1), 2013.

[24] Piotr Lampart. Tip leakage flows in turbines. *Task Quarterly*, 10:139–175, 01 2006.

[25] Philip P. Walsh and Paul Fletcher. *Gas Turbine Performance*. Blackwell Science Ltd, 2 edition, 2004.

[26] Saeed Farokhi. *Aircraft Propulsion*. John Wiley & Sons Ltd, 2 edition, 2014.

[27] S.L. Dixon. *Fluid Mechanics, Thermodynamics of Turbomachinery*. Pergamon International Library. Elsevier Science & Technology Books, 1978.

[28] Hany Moustapha, Mark F. Zelesky, Nicholas C. Baines, and David Japikse. *Axial and Radial Turbines*. Concepts ETI, Inc., 2003.

[29] C.H. Sieverding. *Subsonic turbine blading design*. Von Karman Institute for Fluid Dynamics, 1985.

[30] Pamela Bugała. Review of design of high-pressure turbine. *Journal of KONES*, 24:67–76, 09 2017.

[31] Rafael Guédez. Implementation and validation of loss prediction methods to an existing one dimensional axial turbine design program. Master's thesis, KTH School of Industrial Engineering and Management, 2011.

[32] Luca Da Lio, Giovanni Manente, and Andrea Lazzaretto. A mean-line model to predict the design efficiency of radial inflow turbines in organic rankine cycle (orc) systems. *Applied Energy*, 205:187–209, 2017.

[33] D. O'Dowd. *Aero-thermal performance of transonic high-pressure turbine blade tips*. PhD thesis, University of Oxford, 2010.

[34] S. Can Gülen. *Turbine Aero**, page 217–264. Cambridge University Press, 2019.

[35] John W.R. Taylor and John F. Guilmartin. Military aircraft: The jet age.

[36] Electricity explained. how electricity is generated. U.S. Energy Information Administration.

[37] Mukesh Yadav, Ashwin Misra, Aahan Malhotra, and Naveen Kumar. Design and analysis of a high-pressure turbine blade in a jet engine using advanced materials. *Materials Today: Proceedings*, 25:639–645, 2020. 2nd International Conference on Computational and Experimental Methods in Mechanical Engineering.

[38] Mohammad Arabnia. *Aerodynamic Shape Optimization of Axial Turbines in Three Dimensional Flow*. PhD thesis, Concordia University, 2012.

List of Figures

List of Tables